

Distinct cortical-amygdala projections drive reward value encoding and retrieval

Melissa Malvaez¹, Christine Shieh¹, Michael D. Murphy¹, Venuz Y. Greenfield¹ and Kate M. Wassum^{1,2*}

The value of an anticipated rewarding event is a crucial component of the decision to engage in its pursuit. But little is known of the networks responsible for encoding and retrieving this value. By using biosensors and pharmacological manipulations, we found that basolateral amygdala (BLA) glutamatergic activity tracks and mediates encoding and retrieval of the state-dependent incentive value of a palatable food reward. Projection-specific, bidirectional chemogenetic and optogenetic manipulations revealed that the orbitofrontal cortex (OFC) supports the BLA in these processes. Critically, the function of ventrolateral and medial OFC→BLA projections is doubly dissociable. Whereas lateral OFC→BLA projections are necessary and sufficient for encoding of the positive value of a reward, medial OFC→BLA projections are necessary and sufficient for retrieving this value from memory. These data reveal a new circuit for adaptive reward valuation and pursuit and provide insight into the dysfunction in these processes that characterizes myriad psychiatric diseases.

Prospective consideration of the outcomes of potential action choices is crucial to adaptive decision-making. Chief among these considerations is the value of anticipated rewarding events. This incentive information is state dependent; for example, a food outcome is more valuable when hungry than when sated. It is also learned; the value of a specific reward is encoded during its experience in a relevant motivational state¹. Retrieval of the previously encoded value of an anticipated reward allows adaptive reward pursuit decisions. Dysfunction in either the value encoding or retrieval process will lead to aberrant reward pursuit and ill-informed decision-making—cognitive symptoms that characterize myriad psychiatric diseases. Despite their importance to understanding of adaptive and maladaptive behavior, little is known of the neural circuits that support the encoding and retrieval of state-dependent reward value memories.

The BLA has long been known to mediate emotional learning². Accordingly, this structure is necessary for reward value encoding^{3–5}. But little is known of the circuitry supporting the BLA in this function. Whether the BLA participates in retrieving reward value is less clear and has been disputed^{4,5}, and the contribution of the BLA, if any, to active decision-making is uncertain.

Results

BLA glutamate release tracks reward value encoding and retrieval. The BLA has intrinsic glutamatergic activity⁶ and is densely innervated by glutamatergic projections from regions themselves implicated in reward learning and decision-making⁷. Thus, we sought to begin to fill the gaps in knowledge by using electroenzymatic biosensors to characterize BLA glutamate release during reward value encoding and retrieval (Fig. 1a,b). These biosensors allow subsecond, spatially precise, sensitive, and selective measurement of neuronally released glutamate (Supplementary Fig. 1)^{8,9}. We used a behavioral paradigm that allowed us to experimentally isolate reward value encoding from retrieval of that value and from confounding reinforcement processes (Fig. 1a)³.

Rats were trained while relatively sated (4-h food deprivation) on a self-paced two-lever action sequence to earn sucrose, wherein pressing a ‘seeking’ lever introduced a ‘taking’ lever, a press on which retracted this lever and triggered sucrose delivery. In the sated state, the sucrose has a low value and supports a low rate of lever pressing. Once baseline performance was stable, rats were reexposed to the sucrose in either the familiar sated state or in a hungry state (20-h food deprivation). Because rats had not previously experienced the sucrose while hungry, the latter provided an incentive learning opportunity to encode the high value of the sucrose in the hungry state. Reexposure was noncontingent and was conducted ‘offline’ (without the levers present) to isolate reward value encoding from reinforcement-related confounds and to prevent caching of value to the seeking and taking actions themselves. The effect of this incentive learning opportunity on rats’ reward pursuit was then tested the following day in a brief lever-pressing probe test. No rewards were delivered during this test to force the retrieval of reward value from memory and to avoid online incentive learning. Seeking presses were the primary measure because they have been shown to be selectively sensitive to learned changes in the value of an anticipated reward and relatively immune to more general motivational processes¹⁰. All rats were hungry for this test, but only rats that had previously experienced the sucrose in the hungry state escalated their reward-seeking actions (Fig. 1c and Supplementary Fig. 2; $t_{10} = 2.50$, $P = 0.03$). This result is consistent with the interpretation that the rats retrieved from memory the encoded higher value of the anticipated sucrose reward and used this information to increase the vigor of its pursuit.

BLA glutamate release was found to track reward value encoding. During reexposure, sucrose consumption triggered a transient increase in BLA glutamate concentration, but only if a new value was being encoded (reexposure when hungry; Fig. 1d,e and Supplementary Fig. 3; time: $F_{2,20} = 5.04$, $P = 0.02$; deprivation: $F_{1,10} = 6.67$, $P = 0.03$; time × deprivation: $F_{2,20} = 4.99$, $P = 0.02$; see also Supplementary Table 1). This response was largest early in reexposure (Supplementary Fig. 4), when incentive learning is

¹Department of Psychology, University of California, Los Angeles, Los Angeles, CA, USA. ²Brain Research Institute, University of California, Los Angeles, Los Angeles, CA, USA. *e-mail: kwassum@ucla.edu

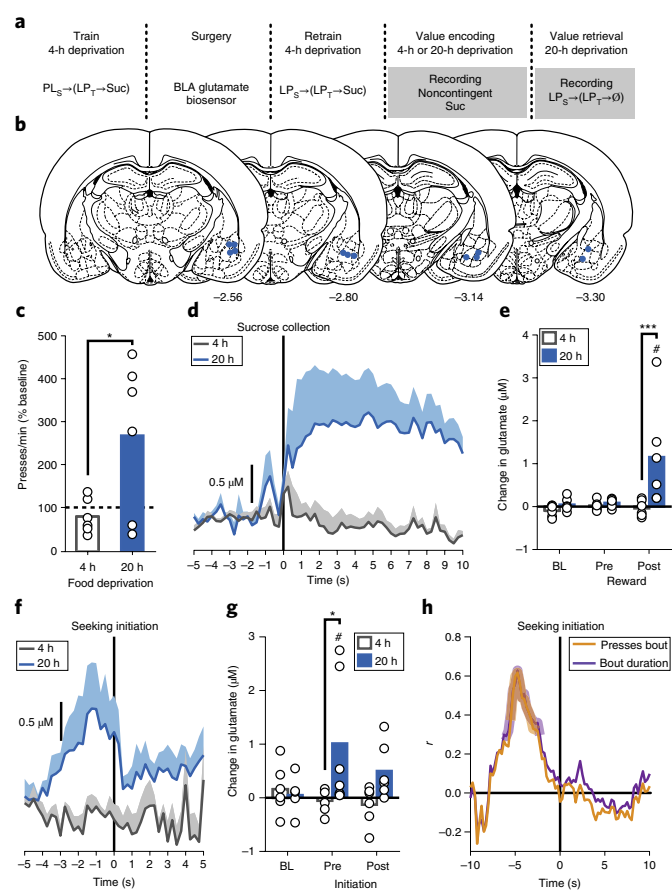


Fig. 1 | BLA glutamate release tracks reward value encoding and retrieval. **a**, Procedure schematic (LP_S, seeking lever press; LP_T, taking lever press; Suc, sucrose; Ø, no sucrose delivered). **b**, Representation of biosensor tip placements. Numbers correspond to anterior-posterior distance (in mm) from bregma. **c**, Reward-seeking press rate (seeking presses/min), normalized to the baseline press rate (average of the last two training sessions conducted following 4-h food deprivation prior to testing; dashed line), during the lever-pressing probe test in the hungry state for rats given prior noncontingent sucrose exposure in a control sated state (4-h food deprivation; no value encoding) or a hungry state (20-h food deprivation; value encoding opportunity) ($N = 6$ rats/group; mean + scatter). Data were analyzed by two-tailed unpaired t test. **d, e**, Trial-averaged BLA glutamate concentration versus time traces (shading reflects between-subjects s.e.m.) (**d**) and quantification (mean + scatter) of the average change in glutamate concentration (**e**) ($N = 6$ biologically independent glutamate recordings/group) prior to (pre) and following (post) sucrose collection/consumption (occurring at time 0 s) or in equivalent baseline periods (BL) during noncontingent sucrose reexposure in sated or hungry rats. Two-way ANOVA was used followed by a Bonferroni-corrected post hoc test for comparison between groups ($***P = 0.0009$) or to baseline ($^{\#}P = 0.002$). **f, g**, Trial-averaged BLA glutamate concentration versus time traces (shading reflects between-subjects s.e.m.) (**f**) and quantification (mean + scatter) of the average change in glutamate concentration (**g**) ($N = 6$ biologically independent glutamate recordings/group) around bout-initiating reward-seeking presses during the lever-pressing probe test in the hungry state. Two-way ANOVA was used followed by a Bonferroni-corrected post hoc test for comparison between groups ($*P = 0.018$) or to baseline ($^{\#}P = 0.026$). **h**, Pearson coefficient ($N = 50$ trials from 6 rats) for correlation between glutamate concentration at each time point around reward-seeking bout initiation and either total seeking presses in or the duration of the subsequent bout. The shaded region indicates significant correlation at $P < 0.05$.

the greatest. There was no BLA glutamate response to the sucrose detectable by the biosensor in the absence of incentive learning, either in the familiar sated state (Fig. 1d,e) or in a familiar hungry state (Supplementary Fig. 5).

BLA glutamate release was also found to track reward value retrieval. In the subsequent lever-pressing test, BLA glutamate transients preceded the initiation of bouts of reward-seeking presses (Supplementary Table 2), but only if rats had prior experience with the sucrose in the hungry state and could therefore retrieve its current value to guide their reward pursuit actions (Fig. 1f,g and Supplementary Fig. 6; time: $F_{2,20} = 1.87$, $P = 0.18$; deprivation: $F_{1,10} = 3.90$, $P = 0.08$; time \times deprivation: $F_{2,20} = 4.31$, $P = 0.03$). BLA glutamate transients selectively preceded the initiation of reward-seeking activity and did not occur prior to subsequent lever presses within a bout (Supplementary Figs. 3d and 6), suggesting that these signals might relate to the considerations driving reward pursuit. This was further supported by evidence that the magnitude of BLA glutamate release before bout initiation positively correlated on a trial-by-trial basis with the number of seeking presses in and the duration of the subsequent bout (presses: $r_{88} = 0.23$, $P = 0.03$; duration: $r_{88} = 0.21$, $P = 0.05$); longer bouts of reward seeking were preceded by larger-amplitude glutamate transients. In the group that received incentive learning, the magnitude of glutamate release significantly predicted future reward-seeking activity in the seconds prior to but not following the initiation of reward seeking (Fig. 1h).

BLA glutamate receptor activity is necessary for reward value encoding and retrieval. We next assessed whether BLA glutamate activity is necessary for encoding and/or retrieval of reward value by blocking BLA glutamate receptors during sucrose reexposure (encoding) or the lever-pressing test following reexposure (retrieval) (Fig. 2). Following training in the sated state, all rats were provided the incentive learning opportunity (sucrose reexposure while hungry; Fig. 2a). Inactivation of NMDA receptors, with ifenprodil⁴¹, or AMPA receptors, with NBQX¹², in the BLA did not in either case alter food-port checking behavior (Fig. 2c; $F_{2,23} = 0.81$, $P = 0.46$) or sucrose palatability responses (Fig. 2d; $F_{2,21} = 0.12$, $P = 0.88$) during reexposure. Inactivation of BLA NMDA but not AMPA receptors did, however, prevent the subsequent upshift in reward seeking that would have otherwise occurred when rats were tested in the hungry state without drug the next day (Fig. 2e and Supplementary Fig. 7; $F_{2,23} = 4.48$, $P = 0.03$), indicating that BLA NMDA receptors are necessary for assigning positive value to a reward. All rats were then given the incentive learning opportunity without drug and were tested again for lever pressing in the hungry state on drug (Fig. 2f). In this case, inactivation of both AMPA and NMDA receptors in the BLA prevented the increase in value-guided reward seeking that should have occurred following incentive learning (Fig. 2g and Supplementary Fig. 8; $F_{2,19} = 7.22$, $P = 0.005$). Therefore, BLA glutamate signaling tracks and is necessary for both reward value encoding and value-guided reward pursuit.

Distinct OFC→BLA projections are necessary for reward value encoding and retrieval. An excitatory input to the BLA might facilitate its function in reward value encoding and retrieval. The OFC is a prime candidate for this because it sends dense glutamatergic innervation to the BLA¹³ and is itself implicated in reward processing and decision-making^{14,15}, including incentive learning¹⁶. Thus, we next used a chemogenetic approach and the same behavioral task to ask whether OFC→BLA projections are necessary for reward value encoding and/or retrieval (Fig. 3). The lateral OFC (lOFC) and medial OFC (mOFC) subdivisions of the OFC are anatomically and functionally distinct^{17,18}. We identified projections to the BLA from both the lOFC and mOFC (Supplementary Fig. 9a,b). Therefore, we assessed the function of both lOFC→BLA and mOFC→BLA projections in reward value encoding and retrieval.

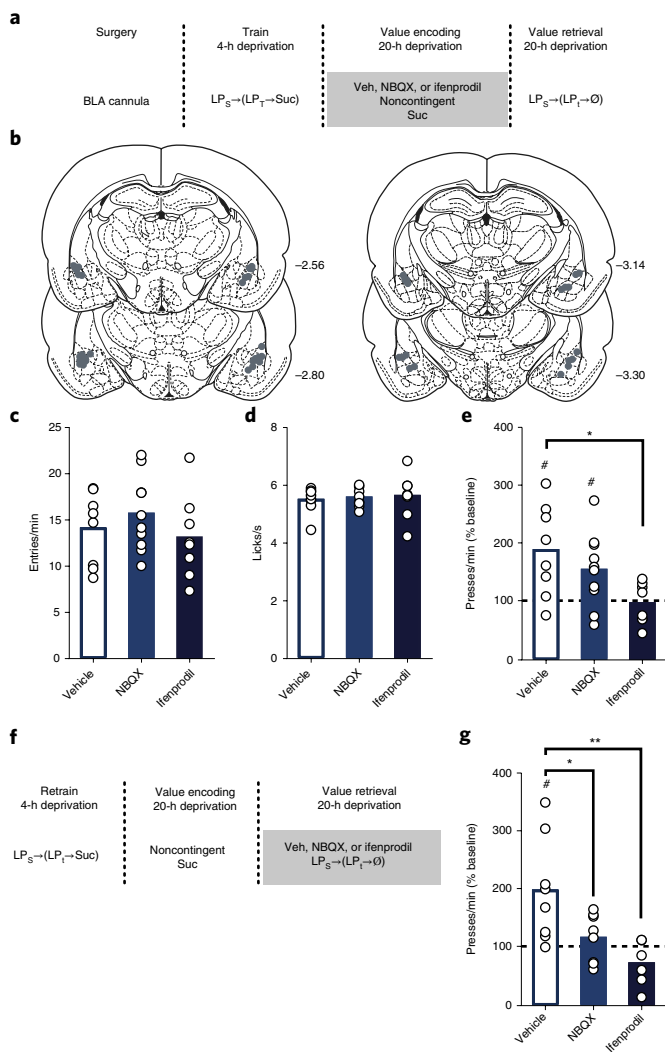


Fig. 2 | BLA glutamate receptor activity is necessary for reward value encoding and retrieval. **a**, Procedure schematic (LP_S , seeking lever press; LP_T , taking lever press; Suc, sucrose; \emptyset , no sucrose delivery; Veh, vehicle; NBQX, AMPA antagonist; ifenprodil, NMDA antagonist). **b**, Microinfusion injector tip placements. Numbers correspond to anterior-posterior distance (in mm) from bregma. **c–e**, Food-port entry rate (entries/min) (**c**) and palatability responses (lick frequency; licks/s) (**d**) during noncontingent sucrose reexposure in the hungry state (20-h food deprivation; value encoding opportunity) following intra-BLA infusion of vehicle ($N=8$ rats), AMPA antagonist ($N=10$ rats), or NMDA antagonist ($N=9$ rats) (analyzed by one-way ANOVA) and subsequent reward-seeking press rate (seeking presses/min), relative to the baseline press rate (dashed line), during a drug-free lever-pressing probe test in the hungry state (analyzed by one-way ANOVA followed by a Bonferroni-corrected post hoc test for comparison between groups ($*P=0.013$) and one-sample t test for comparison to baseline: vehicle, $t_7=3.11$, $\#P=0.017$; NBQX: $t_9=2.63$, $\#P=0.027$) (**e**). **f**, Procedure schematic. **g**, Reward-seeking press rate, relative to baseline (dashed line), during the on-drug (intra-BLA vehicle ($N=8$ rats), AMPA antagonist ($N=8$ rats), or NMDA antagonist ($N=7$ rats)) lever-pressing probe test in the hungry state following off-drug sucrose reexposure in the hungry state (analyzed by one-way ANOVA followed by a Bonferroni-corrected post hoc test for comparison between groups ($*P=0.038$, $**P=0.003$) and one-sample t test for comparison to baseline (vehicle, $t_7=3.021$, $\#P=0.019$)). Data are presented as mean + scatter.

Rats expressing the inhibitory designer receptor human M4 muscarinic receptor (hM4D(Gi)) in excitatory cells of either the IOFC or mOFC showed robust expression in terminals in the

BLA in the vicinity of implanted guide cannulae (Fig. 3b,c; see also Supplementary Fig. 9c,d). Clozapine *N*-oxide (CNO; 1 mM in 0.5 μ l) was infused into the BLA to inactivate these terminals (Supplementary Fig. 10)¹⁹ during the sucrose reexposure incentive learning opportunity and lever pressing was assessed the following day without drug (Fig. 3a). Neither manipulation altered food-port checking behavior (Fig. 3d; $F_{2,26}=0.54$, $P=0.59$) or sucrose palatability responses (Fig. 3e; $F_{2,26}=1.33$, $P=0.28$) online during reexposure. Inhibition of IOFC but not mOFC terminals in the BLA did, however, prevent the subsequent upshift in reward seeking that would have otherwise occurred (Fig. 3f and Supplementary Fig. 11; $F_{2,26}=5.06$, $P=0.014$). These data suggest that activity in IOFC→BLA but not mOFC→BLA projections is necessary for encoding the positive value of a rewarding event.

To determine whether OFC→BLA projections are necessary for reward value retrieval, we allowed all rats to encode the sucrose's high value in the hungry state without drug and then evaluated their lever pressing in the hungry state following intra-BLA vehicle or CNO infusion (Fig. 3g). In this case, inhibition of mOFC but not IOFC terminals in the BLA attenuated reward-seeking activity (Fig. 3h and Supplementary Fig. 12; $F_{2,25}=9.81$, $P=0.0007$), without altering the performance of other indices of motivated behavior (Supplementary Fig. 12). Inactivation of mOFC→BLA projections was without effect if reward value was not being retrieved from memory, either because it had not been learned or because it was observable to the subject and could therefore be held in working memory at test (Supplementary Fig. 13). These data indicate the necessity of activity in mOFC→BLA but not IOFC→BLA projections for retrieving the value of an anticipated reward. Thus, IOFC→BLA projections are necessary for encoding reward value, but their activity is not necessary to retrieve this information. In contrast, mOFC→BLA projections are not necessary for encoding a reward's value but are required to retrieve this information to guide reward pursuit. Secondly, this double dissociation indicates that behavioral effects are not due to off-target effects of CNO itself in the absence of hM4D(Gi), which would cause uniform behavioral effects regardless of the subregion in which hM4D(Gi) was expressed.

Optical stimulation of IOFC→BLA but not mOFC→BLA projections is sufficient to instantiate value to a specific reward. The finding that IOFC→BLA projections were necessary for encoding of positive reward value suggests that activity in these projections might drive such encoding. To test this possibility, we optically stimulated IOFC terminals in the BLA (Supplementary Fig. 10) concurrently with sucrose experience under conditions in which incentive learning would not normally occur: a familiar sated state (Fig. 4a). In a separate group, we stimulated mOFC terminals in the BLA. We restricted optical stimulation (473 nm, 20 Hz, 10 mW, 5 s) to the time of sucrose consumption during noncontingent exposure to match the timing of BLA glutamate release detected during incentive learning (Fig. 1d). Rats expressing the excitatory opsin channelrhodopsin-2 (ChR2) in excitatory cells of either the IOFC or mOFC showed robust expression in terminals in the BLA in the vicinity of implanted optical fibers (Fig. 4b,c; see also Supplementary Fig. 9e,f). Stimulation of IOFC terminals in the BLA concurrently with reward consumption in the familiar sated state did not alter food-port checking behavior (Fig. 4d; $t_{16}=0.20$, $P=0.84$) or sucrose palatability responses (Fig. 4e; $t_{16}=0.25$, $P=0.80$) online. But it did cause a dramatic increase in reward-seeking presses in the test conducted in the same sated state without manipulation the following day (Fig. 4f and Supplementary Fig. 14; $F_{2,24}=9.25$, $P=0.001$), mimicking the effect of hunger-induced incentive learning (Supplementary Fig. 15). This did not occur under otherwise identical circumstances in which stimulation was paired with a task-irrelevant rewarding event (a food pellet), ruling out the confounding possibility of enhanced context salience or other factors unrelated

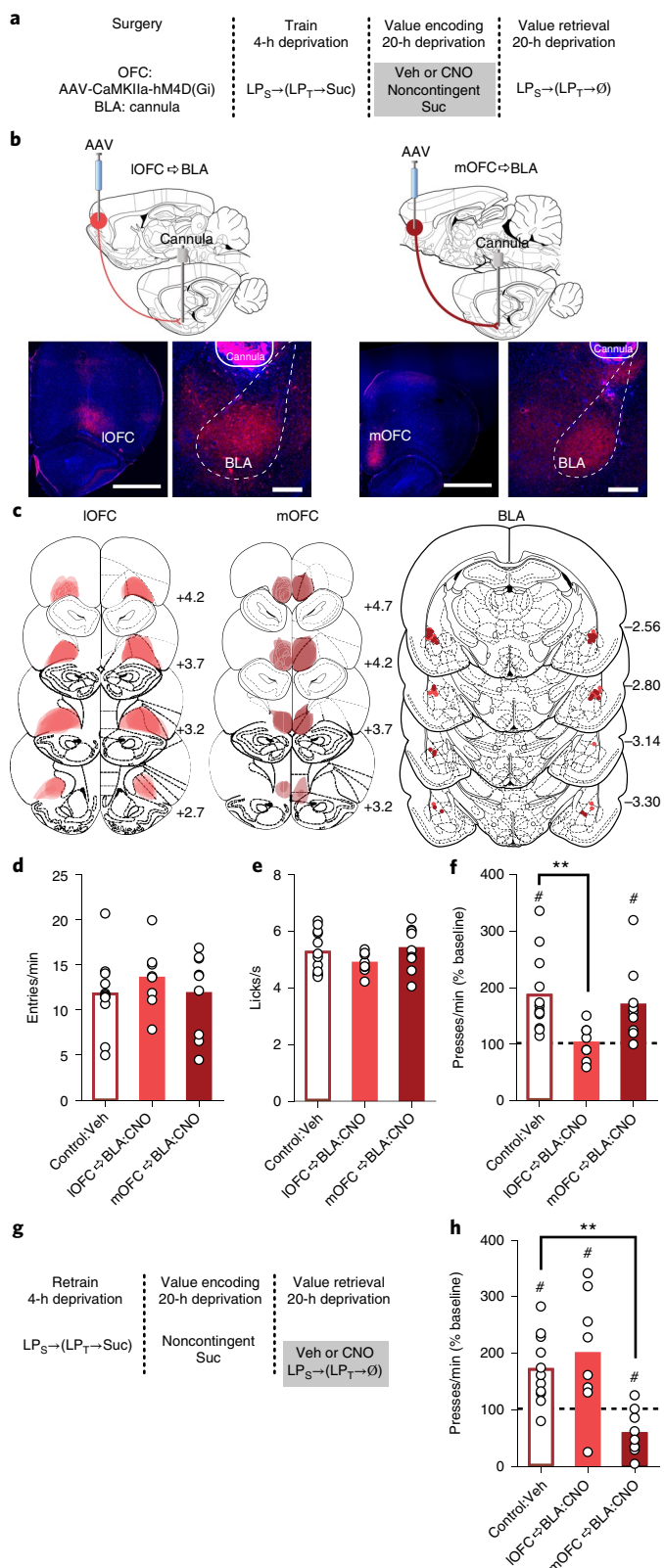
to motivation to obtain the specific anticipated sucrose reward (Fig. 4f). IOFC→BLA stimulation also amplified normal hunger-induced incentive learning (Supplementary Fig. 15). Identical stimulation of mOFC terminals in the BLA had no effect on online food-port checking behavior (Fig. 4d; $t_{10}=0.49$, $P=0.64$) or sucrose palatability responses (Fig. 4e; $t_{10}=0.07$, $P=0.95$), or on subsequent reward-seeking presses (Fig. 4f and Supplementary Fig. 14; $t_{10}=1.17$, $P=0.27$). Thus, activity in IOFC→BLA but not mOFC→BLA projections is sufficient to instantiate value to a rewarding event and thereby drive escalation of its pursuit.

Optical stimulation of mOFC→BLA but not IOFC→BLA projections is sufficient to facilitate reward value retrieval. The finding that mOFC→BLA projections were necessary for reward value retrieval suggests that their activity might facilitate retrieval of the value of an anticipated reward. If this is true, then optically stimulating mOFC→BLA projections during lever pressing should enhance reward seeking following an incentive learning opportunity that would not in itself support an upshift in reward pursuit. To test this possibility, we expressed ChR2 in the mOFC and, following sucrose reexposure in a moderate-hunger state (8-h food deprivation), optically stimulated mOFC terminals in the BLA during a lever-pressing test conducted in the same moderate-hunger state (Fig. 5a–c). A separate group received stimulation of IOFC terminals in the BLA. In controls, sucrose exposure following 8-h food deprivation was not sufficient to drive increased reward pursuit when rats were tested in this state the following day, confirming subthreshold incentive learning (Fig. 5d). Stimulation of mOFC terminals in the BLA (473 nm, 20 Hz, 10 mW, 3 s, once per minute) promoted reward-seeking activity under these conditions (Fig. 5d and Supplementary

Fig. 16; $t_{15}=3.62$, $P=0.003$). Stimulation did not increase reward seeking when rats were tested in the well-learned low-value sated state or following effective incentive learning in the high-value hungry state (Supplementary Fig. 17). mOFC→BLA stimulation was also without effect under otherwise identical circumstances in the absence of the subthreshold incentive learning opportunity (Fig. 5e,f and Supplementary Fig. 18; $t_8=0.67$, $P=0.52$), isolating

Fig. 3 | IOFC→BLA and mOFC→BLA projections are necessary for reward value encoding and retrieval, respectively.

a, Procedure schematic (LP_S, seeking lever press; LP_T, taking lever press; Suc, sucrose; Ø, no sucrose delivery; Veh, vehicle; CNO, clozapine *N*-oxide). **b**, Top: schematic of the chemogenetic approach for inactivation of IOFC (left) and mOFC (right) terminals in the BLA. Bottom: representative immunofluorescence images of HA-tagged hM4D(Gi) expression in IOFC (left; scale bar, 1 mm) and mOFC (right; scale bar, 1 mm) and of cannulae above terminals with expression in the BLA (scale bars, 500 µm). **c**, Schematic representations of hM4D(Gi) expression in IOFC or mOFC and placement of microinfusion injector tips in the BLA for all subjects. Numbers correspond to anterior-posterior distance (in mm) from bregma. **d–f**, Food-port entry rate (entries/min) (**d**) and palatability responses (lick frequency; licks/s) (**e**) during noncontingent sucrose reexposure in the hungry state (20-h food deprivation; value encoding opportunity) following intra-BLA infusion of vehicle ($N=12$ rats, 6 with mOFC hM4D(Gi) expression and 6 with IOFC hM4D(Gi) expression) or CNO (1 mM in 0.5 µl; IOFC→BLA:CNO, $N=8$ rats; mOFC→BLA:CNO, $N=9$ rats; data analyzed by one-way ANOVA) and subsequent reward-seeking press rate (seeking presses/min), relative to the baseline press rate (dashed line), during a drug-free lever-pressing probe test in the hungry state (analyzed by one-way ANOVA followed by a Bonferroni-corrected post hoc test for comparison between groups (** $P=0.009$) and one-sample *t* test for comparison to baseline (control:Veh: $t_{11}=4.36$, $\#P=0.001$; mOFC→BLA:CNO: $t_8=3.07$, $\#P=0.02$) (**f**). **g**, Procedure schematic. **h**, Reward-seeking press rate, relative to the baseline (dashed line), during the on-drug test following off-drug sucrose reexposure in the hungry state, (intra-BLA infusion of vehicle ($N=11$ rats) or CNO (IOFC→BLA:CNO, $N=8$ rats; mOFC→BLA:CNO, $N=9$ rats; data analyzed by one-way ANOVA followed by a Bonferroni-corrected post hoc test for comparison between groups (** $P=0.003$) and one-sample *t* test for comparison to baseline (control:Veh: $t_{10}=3.86$, $\#P=0.003$; IOFC→BLA:CNO: $t_7=2.63$, $\#P=0.03$; mOFC→BLA:CNO: $t_8=3.34$, $\#P=0.01$). ** $P<0.01$, between groups; $\#P<0.05$, relative to baseline. Data are presented as mean + scatter.



its effect to reward value retrieval. Stimulation of IOFC→BLA projections during the reward-seeking test had no effect (Fig. 5d and Supplementary Fig. 16; $t_{11}=0.737$, $P=0.72$). These data indicate that activity in mOFC→BLA but not IOFC→BLA projections is sufficient to facilitate retrieval of a state-dependent reward value. Thus, although it is plausible that optical stimulation of OFC terminals could result in antidromic stimulation of OFC cells that collateralize to cortical or other subcortical targets, these data converge with the data from chemogenetic terminal inactivation (for which antidromic effects have not been reported) to indicate that reward value encoding and retrieval are mediated by IOFC→BLA and mOFC→BLA projections, respectively.

Discussion

These data provide evidence for the BLA as a crucial locus not only for learning about the value of a rewarding event but also for retrieving this information to guide adaptive reward pursuit, identifying it as a critical contributor to value-based decision-making. These value encoding and retrieval functions were found to be supported via doubly dissociable contributions of excitatory input from the IOFC and mOFC. Whereas IOFC→BLA projection activity is necessary and sufficient to drive encoding of a reward's positive value, it does not mediate retrieval of that state-dependent reward value memory. Conversely, activity in mOFC→BLA projections does not mediate reward value encoding but is necessary and sufficient for retrieval of an anticipated reward's value from memory to guide reward pursuit decisions.

BLA glutamate activity was found to track and mediate both reward value encoding and retrieval. The necessity of BLA NMDA receptors for incentive learning is consistent with long-standing knowledge of the crucial role of these receptors in BLA synaptic plasticity^{20,21} and in establishing long-term, BLA-dependent memories^{22,23}. Following a learning event, AMPA receptors are trafficked

to the membrane²⁴ and such trafficking can regulate expression of NMDA-dependent synaptic plasticity in the BLA²⁵. In agreement with this, we found that value-guided reward seeking requires BLA AMPA receptor activation, as well as NMDA receptor activity.

This role for the BLA in reward value encoding and retrieval is in accordance with previous evidence of the necessity of BLA for reward value learning³⁻⁵, but conflicts with data demonstrating that the BLA is not required for value retrieval following sensory-specific satiety devaluation^{4,5}. In these latter experiments, the value shift was negative, temporary, and occurred immediately prior to testing. Our value learning was positive, permanent, and occurred at least 24 h before testing. We suggest therefore that the BLA facilitates encoding and retrieval of long-term, need-state-dependent reward value memories and, as such, is a critical contributor to value-based decision-making. This interpretation is consistent with evidence from humans and nonhuman primates that BLA activity can encode value²⁶, prospectively reflect goal plans²⁷, and predict behavioral choices²⁸ and with evidence of temporally specific BLA inactivation disrupting choice behavior²⁹.

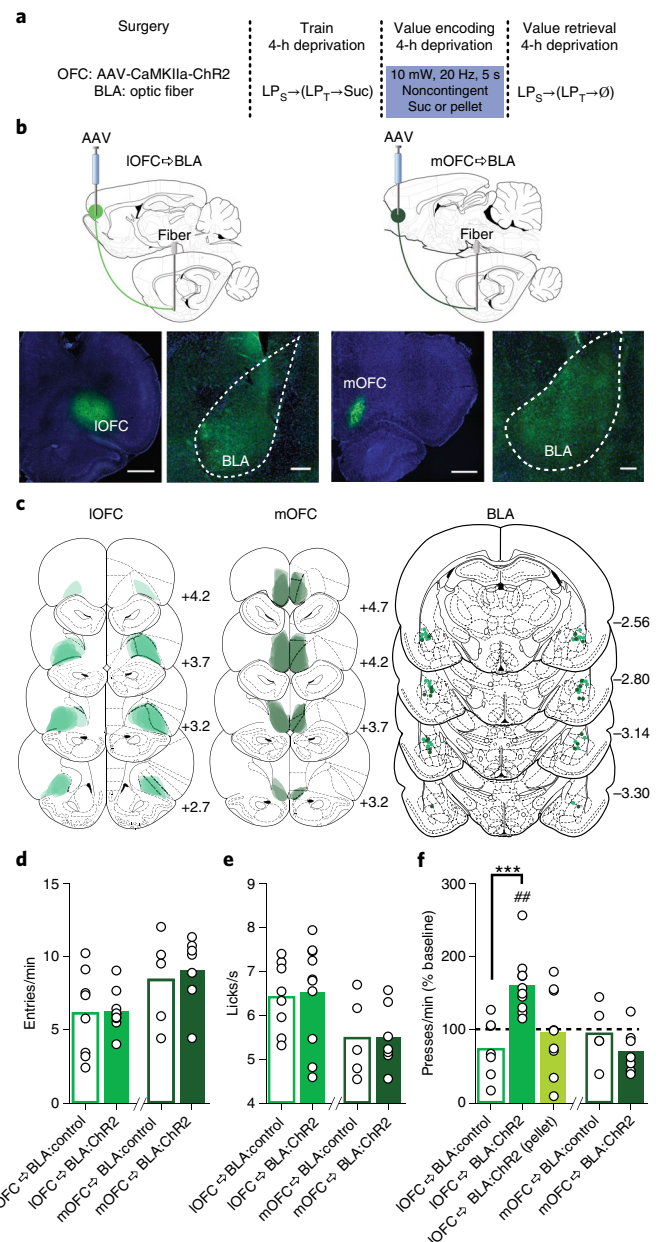


Fig. 4 | Optical stimulation of IOFC terminals in BLA concurrently with reward experience is sufficient to drive positive value assignment.

a, Procedure schematic (LP_S, seeking lever press; LP_T, taking lever press; Suc, sucrose; ∅, no sucrose delivery). **b**, Top: schematic of the optogenetic approach for stimulation of IOFC (left) and mOFC (right) terminals in the BLA. Bottom: representative fluorescence images of Chr2-eYFP expression in IOFC (left; scale bar, 1 mm) and mOFC (right; scale bar, 1 mm) and in the BLA terminal field (scale bars, 250 μm). **c**, Schematic representation of Chr2 expression in IOFC or mOFC and placement of optical fiber tips in BLA for all subjects. Numbers correspond to anterior-posterior distance (in mm) from bregma. **d**, **e**, Food-port entry rate (entries/min) (**d**) and palatability responses (lick frequency; licks/s) (**e**) during noncontingent sucrose reexposure in the control sated state (4-h food deprivation). Light (10 mW, 20 Hz, 5 s) was delivered concurrently with each sucrose collection. Control groups consisted of half eYFP-only rats with 473-nm light delivery and half ChR2-expressing rats with 589-nm light delivery. IOFC→BLA and mOFC→BLA data were analyzed separately by two-tailed unpaired t test. IOFC→BLA:control, $N=8$ rats; IOFC→BLA:ChR2, $N=10$ rats; mOFC→BLA:control, $N=5$ rats; mOFC→BLA:ChR2, $N=7$ rats. **f**, Reward-seeking press rate (seeking presses/min), relative to the baseline press rate (dashed line), during a manipulation-free lever-pressing probe test in the sated state. 'Pellet' refers to the control condition of optical stimulation of IOFC terminals in BLA paired with collection of a task-irrelevant food pellet rather than sucrose. IOFC→BLA data were analyzed by one-way ANOVA followed by a Bonferroni-corrected post hoc test for comparison between groups (*** $P=0.0009$) and one-sample t test for comparison to baseline (IOFC→BLA:ChR2, $t_9=4.84$, $\#P=0.0009$); mOFC→BLA data were analyzed by two-tailed unpaired t test. IOFC→BLA:control, $N=8$ rats; IOFC→BLA:ChR2, $N=10$ rats; IOFC→BLA:ChR2 (pellet), $N=9$ rats; mOFC→BLA:control, $N=5$ rats; mOFC→BLA:ChR2, $N=7$ rats. Data are presented as mean + scatter.

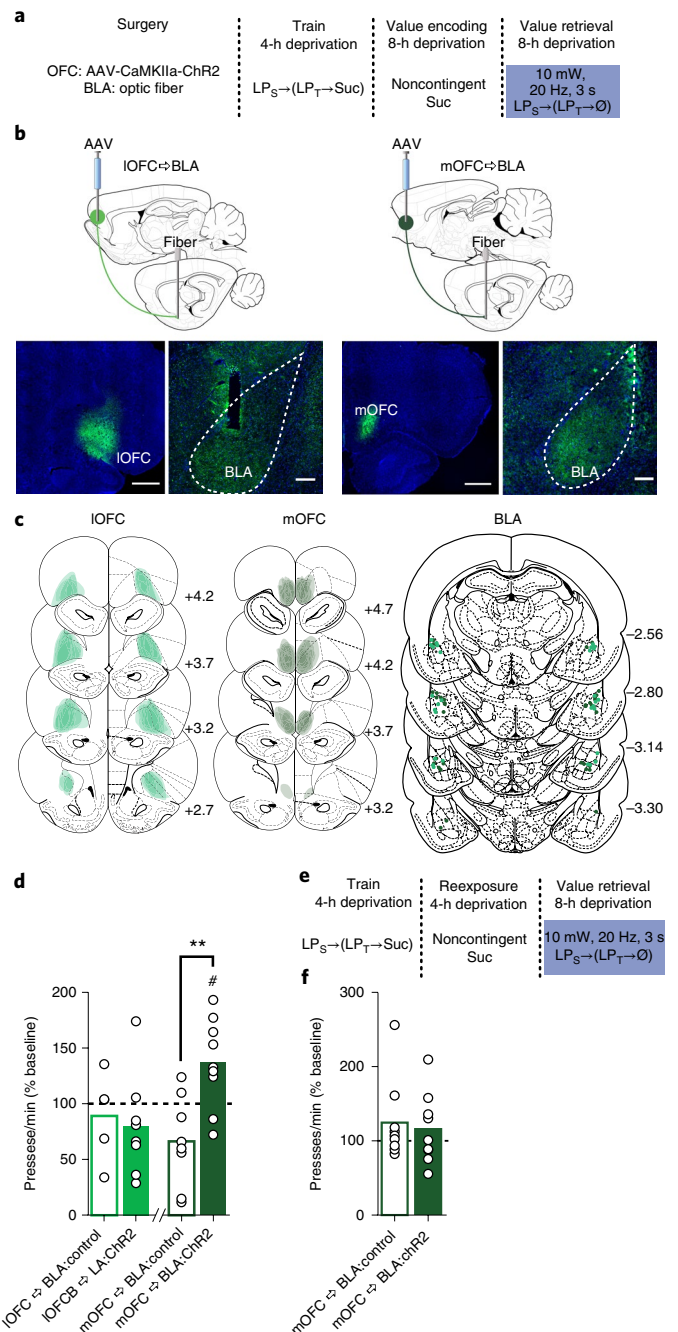
BLA input from the IOFC but not the mOFC was found to mediate reward value encoding. This is consistent with recent evidence that the IOFC itself is necessary for both positive and negative incentive learning¹⁶ and with evidence that IOFC lesions disrupt sensitivity of reward seeking to outcome devaluation³⁰. It is also in line with evidence in human IOFC of reward identity coding that is sensitive to reward value shifts^{31,32} and identity-based reward value coding³³. Interestingly, IOFC→BLA manipulation altered reward value encoding without concomitant changes in the palatability response to the reward, in line with previous evidence of the dissociability of these processes³.

The finding that activity at both glutamatergic IOFC terminals and the NMDA receptors known to mediate synaptic plasticity in the BLA is necessary for reward value encoding suggests that IOFC→BLA projections might direct encoding of reward value in the BLA. In agreement with this, an intact IOFC is required for the BLA to encode information about expected outcomes³⁴. Stimulation of IOFC→BLA projections concurrently with reward experience augmented later reward pursuit. Thus, IOFC→BLA projections may convey value to the BLA. However, this should not rule out a function for the OFC in retaining some forms of reward memory. The IOFC has itself been implicated in the retention and perhaps consolidation of action–outcome memories^{35,36}.

Surprisingly, whereas IOFC→BLA projections were found to mediate reward value encoding, IOFC→BLA activity was neither necessary nor sufficient for retrieval of this memory during reward pursuit. Rather, mOFC→BLA projections were found to mediate retrieval of state-dependent reward value memories. Thus, the activity of mOFC→BLA projections is critical to ensure reward pursuit commensurate with one's current state. This is consistent with evidence that the mOFC itself mediates effort allocation according to anticipated reward value³⁷, outcome anticipation³⁸, and other aspects of reward-related decision-making^{39,40}. Confirming that

mOFC→BLA projections mediate reward value retrieval, rather than having broader function in reward-related behavior, manipulation of mOFC→BLA projections only altered reward pursuit if a state-dependent reward value had been encoded. mOFC→BLA manipulations were without effect in the absence of incentive learning. Moreover, stimulation of mOFC→BLA projections only augmented reward seeking if the internal state was not sufficiently discriminable on its own to support enhanced reward pursuit following incentive learning. Thus, rather than conveying a value signal itself to the BLA, which would result in increased reward seeking regardless of prior learning or state, mOFC→BLA projections facilitate retrieval of reward value, which may be stored in the BLA or downstream.

Both the IOFC and mOFC have been proposed to be involved in representing and using information about current and anticipated



states or situations to guide adaptive behavior when the information defining those states (for example, an anticipated reward and its value) is 'hidden', or not readily externally observable^{38,41}. For example, the mOFC is necessary for anticipating potential rewarding outcomes and acting accordingly when such outcomes are not present, but it is not required when rewards are present to guide decision-making³⁸. Adaptive behavior in our task relies on such a hidden state representation. Although there has been no perceptual change following incentive learning (same context, levers, etc.), the state is nonetheless different: the anticipated reward is now more valuable. The critical elements defining this state—internal need and the reward itself—are not externally perceptible. Our data therefore indicate that IOFC→BLA and mOFC→BLA projections mediate encoding and retrieval, respectively, of the state-dependent incentive value of a specific anticipated reward.

The demonstrated doubly dissociable function of IOFC→BLA and mOFC→BLA projections in encoding and retrieving, respectively, a reward's value is consistent with some recent evidence from primates of similarly dissociable IOFC and mOFC function. The primate IOFC has been shown to be involved in credit assignment^{17,42} and value updating following devaluation⁴³. In contrast, primate mOFC has been implicated in value-guided decision-making^{17,42}. The present results translate this dissociability to rodents and, by using bidirectional, projection-specific manipulations, suggest that these functions are achieved, at least in part, via projections to the BLA, which are conserved between rat and primates¹³.

One critical new question is which BLA projections mediate the encoding and retrieval of reward value. Among other potential targets, the BLA might relay this information back to the OFC. Both the IOFC and mOFC have been implicated in choice and reward-seeking behavior^{18,44,45} and, whereas some subregions of the primate IOFC are important for updating reward value, in agreement with our findings, others have been demonstrated to be necessary for goal selection following a value shift⁴³. Indeed, direct BLA→IOFC projections are necessary for retrieving specific cue-triggered reward memories¹⁹. IOFC and mOFC terminals were found to overlap extensively in the BLA; thus, regardless of which BLA neurons mediate reward value memory, the IOFC and mOFC inputs are positioned to target the same network of BLA cells.

These data reveal many other questions ripe for future exploration. For example, whether OFC projections to other cortical or subcortical targets also regulate reward value encoding and retrieval remains unknown. The contribution of IOFC→BLA/mOFC→BLA circuitry to other forms of memory is another important area to address. Indeed, like the BLA², the OFC functions in both appetitive and aversive behavior^{36,46} and an intact OFC is necessary for the BLA to encode predicted appetitive or aversive outcomes³⁴. The possibility that the organizing principle exposed by these data applies to other memory systems is also intriguing.

The finding that reward value encoding and retrieval were functionally and neuroanatomically dissociable reveals a clear vulnerability in the brain for poor decision-making. Moreover, we found that positive reward valuation could be prevented or induced without concomitant changes in the palatability responses indicative of a reward's emotional experience. OFC–BLA circuitry is known to become dysfunctional in patients diagnosed with addiction⁴⁷, anxiety⁴⁸, depression⁴⁹, and schizophrenia⁵⁰. The current data therefore provide insight into how cortical amygdala dysfunction might contribute to these and other psychiatric diseases characterized by maladaptive reward valuation and poor reward-related decision-making.

Online content

Any methods, additional references, Nature Research reporting summaries, source data, statements of data availability and associated accession codes are available at <https://doi.org/10.1038/s41593-019-0374-7>.

Received: 27 April 2018; Accepted: 28 February 2019;
Published online: 8 April 2019

References

- Dickinson, A. & Balleine, B. W. Motivational control over goal-directed action. *Anim. Learn. Behav.* **22**, 1–18 (1994).
- Wassum, K. M. & Izquierdo, A. The basolateral amygdala in reward learning and addiction. *Neurosci. Biobehav. Rev.* **57**, 271–283 (2015).
- Wassum, K. M., Ostlund, S. B., Maidment, N. T. & Balleine, B. W. Distinct opioid circuits determine the palatability and the desirability of rewarding events. *Proc. Natl Acad. Sci. USA* **106**, 12512–12517 (2009).
- Parkes, S. L. & Balleine, B. W. Incentive memory: evidence the basolateral amygdala encodes and the insular cortex retrieves outcome values to guide choice between goal-directed actions. *J. Neurosci.* **33**, 8753–8763 (2013).
- West, E. A. et al. Transient inactivation of basolateral amygdala during selective satiation disrupts reinforcer devaluation in rats. *Behav. Neurosci.* **126**, 563–574 (2012).
- Pitkänen, A., Savander, M., Nurminen, N. & Ylinen, A. Intrinsic synaptic circuitry of the amygdala. *Ann. NY Acad. Sci.* **985**, 34–49 (2003).
- Price, J. L. Definition of the orbital cortex in relation to specific connections with limbic and visceral structures and other cortical regions. *Ann. NY Acad. Sci.* **1121**, 54–71 (2007).
- Wassum, K. M. et al. Transient extracellular glutamate events in the basolateral amygdala track reward-seeking actions. *J. Neurosci.* **32**, 2734–2746 (2012).
- Malvaez, M. et al. Basolateral amygdala rapid glutamate release encodes an outcome-specific representation vital for reward-predictive cues to selectively invigorate reward-seeking actions. *Sci. Rep.* **5**, 12511 (2015).
- Balleine, B. W., Garner, C., Gonzalez, F. & Dickinson, A. Motivational control of heterogeneous instrumental chains. *J. Exp. Psychol. Anim. Behav. Process.* **21**, 203–217 (1995).
- Williams, K. Ifenprodil discriminates subtypes of the N-methyl-D-aspartate receptor: selectivity and mechanisms at recombinant heteromeric receptors. *Mol. Pharmacol.* **44**, 851–859 (1993).
- Sheardown, M. J., Nielsen, E. O., Hansen, A. J., Jacobsen, P. & Honoré, T. 2,3-Dihydroxy-6-nitro-7-sulfamoyl-benzo(F)quinoxaline: a neuroprotectant for cerebral ischemia. *Science* **247**, 571–574 (1990).
- Heilbronner, S. R., Rodriguez-Romaguera, J., Quirk, G. J., Groenewegen, H. J. & Haber, S. N. Circuit-based corticostriatal homologies between rat and primate. *Biol. Psychiatry* **80**, 509–521 (2016).
- Ostlund, S. B. & Balleine, B. W. The contribution of orbitofrontal cortex to action selection. *Ann. NY Acad. Sci.* **1121**, 174–192 (2007).
- Murray, E. A. & Izquierdo, A. Orbitofrontal cortex and amygdala contributions to affect and action in primates. *Ann. NY Acad. Sci.* **1121**, 273–296 (2007).
- Baltz, E. T., Yalcinbas, E. A., Renteria, R. & Gremel, C. M. Orbital frontal cortex updates state-induced value change for decision-making. *eLife* **7**, e35988 (2018).
- Rudebeck, P. H. & Murray, E. A. Balkanizing the primate orbitofrontal cortex: distinct subregions for comparing and contrasting values. *Ann. NY Acad. Sci.* **1239**, 1–13 (2011).
- Izquierdo, A. Functional heterogeneity within rat orbitofrontal cortex in reward learning and decision making. *J. Neurosci.* **37**, 10529–10540 (2017).
- Lichtenberg, N. T. et al. Basolateral amygdala to orbitofrontal cortex projections enable cue-triggered reward expectations. *J. Neurosci.* **37**, 8374–8384 (2017).
- Bauer, E. P., Schafe, G. E. & LeDoux, J. E. NMDA receptors and L-type voltage-gated calcium channels contribute to long-term potentiation and different components of fear memory formation in the lateral amygdala. *J. Neurosci.* **22**, 5239–5249 (2002).
- Müller, T., Albrecht, D. & Gebhardt, C. Both NR2A and NR2B subunits of the NMDA receptor are critical for long-term potentiation and long-term depression in the lateral amygdala of horizontal slices of adult mice. *Learn. Mem.* **16**, 395–405 (2009).
- Riedel, G., Platt, B. & Micheau, J. Glutamate receptor function in learning and memory. *Behav. Brain Res.* **140**, 1–47 (2003).
- Rodrigues, S. M., Schafe, G. E. & LeDoux, J. E. Intra-amygdala blockade of the NR2B subunit of the NMDA receptor disrupts the acquisition but not the expression of fear conditioning. *J. Neurosci.* **21**, 6889–6896 (2001).
- Malinow, R. & Malenka, R. C. AMPA receptor trafficking and synaptic plasticity. *Annu. Rev. Neurosci.* **25**, 103–126 (2002).
- Yu, S. Y., Wu, D. C., Liu, L., Ge, Y. & Wang, Y. T. Role of AMPA receptor trafficking in NMDA receptor-dependent synaptic plasticity in the rat lateral amygdala. *J. Neurochem.* **106**, 889–899 (2008).
- Jenison, R. L., Rangel, A., Oya, H., Kawasaki, H. & Howard, M. A. Value encoding in single neurons in the human amygdala during decision making. *J. Neurosci.* **31**, 331–338 (2011).

27. Hernádi, I., Grabenhorst, F. & Schultz, W. Planning activity for internally generated reward goals in monkey amygdala neurons. *Nat. Neurosci.* **18**, 461–469 (2015).
28. Grabenhorst, F., Hernádi, I. & Schultz, W. Prediction of economic choice by primate amygdala neurons. *Proc. Natl Acad. Sci. USA* **109**, 18950–18955 (2012).
29. Orsini, C. A. et al. Optogenetic inhibition reveals distinct roles for basolateral amygdala activity at discrete time points during risky decision making. *J. Neurosci.* **37**, 11537–11548 (2017).
30. Gremel, C. M. & Costa, R. M. Orbitofrontal and striatal circuits dynamically encode the shift between goal-directed and habitual actions. *Nat. Commun.* **4**, 2264 (2013).
31. Howard, J. D., Gottfried, J. A., Tobler, P. N. & Kahnt, T. Identity-specific coding of future rewards in the human orbitofrontal cortex. *Proc. Natl Acad. Sci. USA* **112**, 5195–5200 (2015).
32. Howard, J. D. & Kahnt, T. Identity-specific reward representations in orbitofrontal cortex are modulated by selective devaluation. *J. Neurosci.* **37**, 2627–2638 (2017).
33. Suzuki, S., Cross, L. & O'Doherty, J. P. Elucidating the underlying components of food valuation in the human orbitofrontal cortex. *Nat. Neurosci.* **20**, 1780–1786 (2017).
34. Saddoris, M. P., Gallagher, M. & Schoenbaum, G. Rapid associative encoding in basolateral amygdala depends on connections with orbitofrontal cortex. *Neuron* **46**, 321–331 (2005).
35. Zimmermann, K. S., Yamin, J. A., Rainnie, D. G., Ressler, K. J. & Gourley, S. L. Connections of the mouse orbitofrontal cortex and regulation of goal-directed action selection by brain-derived neurotrophic factor. *Biol. Psychiatry* **81**, 366–377 (2017).
36. Zimmermann, K. S., Li, C. C., Rainnie, D. G., Ressler, K. J. & Gourley, S. L. Memory retention involves the ventrolateral orbitofrontal cortex: comparison with the basolateral amygdala. *Neuropsychopharmacology* **43**, 674 (2018).
37. Gourley, S. L., Zimmermann, K. S., Allen, A. G. & Taylor, J. R. The medial orbitofrontal cortex regulates sensitivity to outcome value. *J. Neurosci.* **36**, 4600–4613 (2016).
38. Bradfield, L. A., Dezfouli, A., van Holstein, M., Chieng, B. & Balleine, B. W. Medial orbitofrontal cortex mediates outcome retrieval in partially observable task situations. *Neuron* **88**, 1268–1280 (2015).
39. Stopper, C. M., Green, E. B. & Floresco, S. B. Selective involvement by the medial orbitofrontal cortex in biasing risky, but not impulsive, choice. *Cereb. Cortex* **24**, 154–162 (2014).
40. Dalton, G. L., Wang, N. Y., Phillips, A. G. & Floresco, S. B. Multifaceted contributions by different regions of the orbitofrontal and medial prefrontal cortex to probabilistic reversal learning. *J. Neurosci.* **36**, 1996–2006 (2016).
41. Wilson, R. C., Takahashi, Y. K., Schoenbaum, G. & Niv, Y. Orbitofrontal cortex as a cognitive map of task space. *Neuron* **81**, 267–279 (2014).
42. Noonan, M. P., Chau, B. K. H., Rushworth, M. F. S. & Fellows, L. K. Contrasting effects of medial and lateral orbitofrontal cortex lesions on credit assignment and decision-making in humans. *J. Neurosci.* **37**, 7023–7035 (2017).
43. Murray, E. A., Moylan, E. J., Saleem, K. S., Basile, B. M. & Turchi, J. Specialized areas for value updating and goal selection in the primate orbitofrontal cortex. *eLife* **4**, e11695 (2015).
44. Rudebeck, P. H. & Rich, E. L. Orbitofrontal cortex. *Curr. Biol.* **28**, R1083–R1088 (2018).
45. Murray, E. A. & Rudebeck, P. H. Specializations for reward-guided decision-making in the primate ventral prefrontal cortex. *Nat. Rev. Neurosci.* **19**, 404–417 (2018).
46. Plassmann, H., O'Doherty, J. P. & Rangel, A. Appetitive and aversive goal values are encoded in the medial orbitofrontal cortex at the time of decision making. *J. Neurosci.* **30**, 10799–10808 (2010).
47. Volkow, N. D. & Fowler, J. S. Addiction, a disease of compulsion and drive: involvement of the orbitofrontal cortex. *Cereb. Cortex* **10**, 318–325 (2000).
48. Sladky, R. et al. Disrupted effective connectivity between the amygdala and orbitofrontal cortex in social anxiety disorder during emotion discrimination revealed by dynamic causal modeling for fMRI. *Cereb. Cortex* **25**, 895–903 (2015).
49. Price, J. L. & Drevets, W. C. Neurocircuitry of mood disorders. *Neuropsychopharmacology* **35**, 192–216 (2010).
50. Liu, H. et al. Differentiating patterns of amygdala–frontal functional connectivity in schizophrenia and bipolar disorder. *Schizophr. Bull.* **40**, 469–477 (2014).

Acknowledgements

This research was supported by NIH grants DA035443, MH106972, and NS087494 to K.M.W. and NIH grants DA038942 and DA024635 to M.M. We acknowledge helpful feedback from N. Lichtenberg and A. Izquierdo on these data and this manuscript.

Author contributions

M.M. and K.M.W. designed the research and analyzed and interpreted the data. M.M. conducted the research with assistance from C.S., M.D.M., and V.Y.G. M.M. and K.M.W. wrote the manuscript.

Competing interests

The authors declare no competing interests.

Additional information

Supplementary information is available for this paper at <https://doi.org/10.1038/s41593-019-0374-7>.

Reprints and permissions information is available at www.nature.com/reprints.

Correspondence and requests for materials should be addressed to K.M.W.

Publisher's note: Springer Nature remains neutral with regard to jurisdictional claims in published maps and institutional affiliations.

© The Author(s), under exclusive licence to Springer Nature America, Inc. 2019

Methods

Subjects. Male Long Evans rats (aged 8–10 weeks at the start of the experiment; Charles River Laboratories) were group housed and handled for 3–5 d prior to the start of the experiment. Unless otherwise noted, separate groups of naive rats were used for each experiment. Rats were provided with water ad libitum in the home cage and were maintained on food restriction for a certain amount of time each day, as described below. Experiments were performed during the dark phase of a reverse 12-h dark/12-h light cycle. All procedures were conducted in accordance with the NIH Guide for the Care and Use of Laboratory Animals and were approved by the UCLA Institutional Animal Care and Use Committee.

Surgery. Standard surgical procedures described previously⁹ were used for all surgeries. Rats were anesthetized with isoflurane (4–5% induction, 1–2% maintenance), and a nonsteroidal anti-inflammatory agent was administered pre- and postoperatively to minimize pain and discomfort. Following surgery, rats were individually housed.

Electroenzymatic glutamate recordings. Following training to stable performance, rats were implanted with a unilateral precalibrated glutamate biosensor in the BLA (AP –3.0 mm, ML +5.1 mm, DV –8.0 mm) and an Ag/AgCl reference electrode in the contralateral cortex. Biosensor placement was verified by standard histological procedures (Fig. 1b).

BLA glutamate receptor inactivation. Following training to stable performance, rats were implanted with a guide cannula (22 gauge, stainless steel; Plastics One) targeted bilaterally 1 mm above the BLA (AP –3.0 mm, ML ±5.1 mm, DV –7.0 mm). Cannula placement was verified by standard histological procedures (Fig. 1b) and subjects were removed from the study if placement was off-target ($N = 1$).

Chemogenetic manipulation of OFC→BLA projections. Prior to onset of behavioral training, rats were randomly assigned to an OFC subregion group, anesthetized with isoflurane, and infused bilaterally with adeno-associated virus (AAV) expressing the inhibitory designer receptor hM4D(Gi) (AAV8-CaMKIIa-HA-hM4D(Gi)-IRES-mCitrine). Virus (0.30 μ l) was infused at a rate of 6 μ l/h via an infusion needle positioned in the IOFC (AP +3.2 mm, ML ±2.4 mm, DV –5.4 mm) or mOFC (AP +4.0 mm, ML ±0.5 mm, DV –5.2 mm). Bilateral guide cannulae (22 gauge, stainless steel; Plastics One) were implanted 1 mm above the BLA (AP –3.0 mm, ML ±5.1 mm, DV –7.0 mm). Testing commenced 8 weeks after surgery to ensure axonal transport and expression in IOFC or mOFC terminals in the BLA. Restriction of expression to the IOFC or mOFC was verified with immunofluorescence by using an antibody recognizing the HA tag. Cannula placements in the terminal expression region were verified by standard histological procedures. Subjects were removed from the study if they lacked expression or if cannulae were misplaced outside the BLA (IOFC, $N = 0$; mOFC, $N = 2$).

Optogenetic manipulation of OFC→BLA projections. Prior to onset of behavioral training, rats were randomly assigned to a viral group, anesthetized with isoflurane, and infused bilaterally with AAV expressing the excitatory opsin ChR2 (AAV5-CaMKIIa-hChR2(H134R)-eYFP) or the enhanced yellow fluorescent protein (eYFP) control (AAV8-CaMKIIa-eYFP). Virus (0.30 μ l) was infused at a rate of 6 μ l/h via an infusion needle positioned in the IOFC or mOFC. Bilateral optical fibers (200- μ m core, numerical aperture of 0.66; Prizmatix) held in ferrules (Kientec Systems) were implanted 0.3 mm above the BLA (AP –3.0 mm, ML ±5.1 mm, DV –7.7 mm). Testing commenced 8 weeks after surgery to ensure axonal transport and expression in IOFC or mOFC terminals in the BLA. Restriction of virus to either the IOFC or mOFC was verified with eYFP fluorescence, and optical fiber placements in the vicinity of terminal expression were verified by standard histological procedures. Subjects were removed from the study if they lacked expression or if optical fibers were misplaced outside the BLA (IOFC, $N = 1$; mOFC, $N = 1$).

Validation of chemogenetic and optogenetic manipulation of OFC→BLA projections. hM4d(Gi) and ChR2 were coexpressed by infusing AAV5-CaMKIIa-hChR2(H134R)-eYFP and either AAV8-CaMKIIa-HA-hM4D(Gi)-IRES-mCitrine or AAV5-CaMKIIa-mCherry bilaterally into the IOFC (AP +3.2 mm, ML ±2.4 mm, DV –5.4 mm) or mOFC (AP +4.0 mm, ML ±0.5 mm, DV –5.2 mm). Eight weeks after viral infusion, rats were anesthetized and a precalibrated microelectrode array (MEA) glutamate biosensor was affixed to an optical fiber. A guide cannula was acutely implanted into the BLA (AP –3.0 mm, ML +5.1 mm, DV –8.0 mm), and an Ag/AgCl reference electrode was placed in the contralateral cortex. The optical fiber was affixed behind the MEA (to reduce photovoltaic artifacts) and positioned such that the optical fiber tip terminated 0.3 mm above the glutamate-sensing electrodes. The guide cannula (Plastics One) terminated 6.5 mm above the MEA tip to avoid tissue damage and was positioned such that, when inserted, the injector (Plastics One) would protrude 6.2 mm and end within 100 μ m of the microelectrodes. The injector was inserted after the biosensor/optical fiber probe was lowered into the BLA to further minimize tissue damage. The level of anesthesia was kept constant throughout recordings by maintaining a constant breathing rate (1 breath per minute), which was achieved by adjusting the

isoflurane level (1–1.5%). Viral expression was verified by immunofluorescence and biosensor placements were verified by standard histological procedures (Supplementary Fig. 10).

Electroenzymatic glutamate biosensors. *Biosensor fabrication.* MEA probes were fabricated in the Nanoelectronics Research Facility at UCLA and modified for glutamate detection as described previously^{8,9,51}. Briefly, these biosensors use glutamate oxidase (GluOx) as the biological recognition element and rely on electro-oxidation, via constant-potential amperometry (0.7 V versus an Ag/AgCl reference electrode), of enzymatically generated hydrogen peroxide (H_2O_2) reporter molecule to provide a current signal. This current output is recorded and converted to glutamate concentration by a calibration factor determined in vitro. Enzyme immobilization was accomplished by chemical cross-linking with a solution consisting of GluOx, BSA, and glutaraldehyde. Interference from electroactive anions and cations is effectively excluded from amperometric recordings, while still maintaining a subsecond response time, by electropolymerization of polypyrrole (PPY) or poly(*o*-phenylenediamine) (PPD), as well as dip-coat application of Nafion to the electrode sites prior to enzyme immobilization^{8,9,51}. Each MEA had two non-enzyme-coated sentinel electrodes for removal of correlated noise from the glutamate-sensing electrodes by signal subtraction, as described previously^{8,9}. These electrodes were prepared identically with the exception that the BSA and glutaraldehyde solution did not contain GluOx. The average in vivo limit of glutamate detection for the sensors used in this study was 0.36 μ M (s.e.m. = 0.03 μ M, range 0.13–0.67 μ M).

Reagents. Nafion (5% solution in a lower aliphatic alcohols/ H_2O mix), BSA (min 96%), glutaraldehyde (25% in water), pyrrole (98%), *p*-phenylenediamine (98%), L-glutamic acid, L-ascorbic acid, and 3-hydroxytyramine (dopamine) were purchased from Aldrich Chemical Co. L-GluOx from *Streptomyces* sp. X119-6, with a rated activity of 24.9 units per mg protein, produced by Yamasa Corporation, was purchased from US Biological. PBS was composed of 50 mM Na_2HPO_4 with 100 mM NaCl (pH 7.4). Ultrapure water generated with a Millipore Milli-Q Water System (resistivity = 18 $M\Omega$ -cm) was used for preparation of all solutions used in this work.

Instrumentation. Electrochemical preparation of the sensors was performed by using a Versatile Multichannel Potentiostat (model VMP3) equipped with the 'p' low-current option and low-current N' stat box (Bio-Logic USA). In vitro and in vivo measurements were conducted with a low-noise multichannel Fast-16 mkIII potentiostat (Quanton), with reference electrodes consisting of a glass-enclosed Ag/AgCl wire in 3 M NaCl solution (Bioanalytical Systems) and a 200- μ m-diameter Ag/AgCl wire, respectively. All potentials are reported with respect to the Ag/AgCl reference electrode. Oxidative current was recorded at 80 kHz and was averaged over 0.25-s intervals.

In vitro biosensor characterization. All biosensors were calibrated in vitro to test for sensitivity and selectivity of glutamate measurement prior to implantation. A constant potential of 0.7 V was applied to the working electrodes against an Ag/AgCl reference electrode in 40 ml of stirred PBS at pH 7.4 and 37 °C in a Faraday cage. After current detected at the electrodes equilibrated (~30–45 min), aliquots of glutamate were added to the beaker to reach final glutamate concentrations in the range of 5–60 μ M. A calibration factor based on these responses was calculated for each GluOx-coated electrode. The average calibration factor for the sensors used in these studies was 135.98 μ M/nA. Control electrodes, coated with PPY or PPD, Nafion, and BSA/glutaraldehyde, but not GluOx, showed no detectable response to glutamate. Aliquots of ascorbic acid (250 μ M final concentration) and dopamine (5–10 μ M final concentration) were added to the beaker as representative examples of readily oxidizable potential anionic and cationic interferent neurochemicals, respectively, to confirm selectivity for glutamate (Supplementary Fig. 1). For the sensors used in these studies, no current changes above the level of noise were detected with the addition of cationic or anionic interferents, as reported previously^{8,9,51}. To assess the uniformity of H_2O_2 sensitivity across control and GluOx-coated electrodes, aliquots of H_2O_2 (10 μ M) were also added to the beaker. There was less than a 10% difference in the H_2O_2 sensitivity on control electrode sites relative to enzyme-coated sites, which was statistically insignificant ($t_{42} = 0.32$, $P = 0.75$), indicating that any changes detected in vivo on enzyme-coated biosensor sites following control channel signal subtraction could not be attributed to endogenous H_2O_2 .

In vivo validation of chemogenetic and optogenetic manipulation of OFC→BLA projections. Glutamate biosensors were used to validate optogenetic stimulation and chemogenetic inhibition of OFC terminals in the BLA. Rats expressing ChR2 and hM4d(Gi) in either the IOFC or mOFC were anesthetized and implanted with a precalibrated MEA-fiber-cannula probe in the BLA, as described above. Experiments were conducted inside a Faraday cage. Following sensor implantation, an injector was inserted into the cannula. A constant potential of 0.7 V was applied to the working electrodes against the Ag/AgCl reference electrode implanted in the contralateral hemisphere. The detected current was allowed to equilibrate (~30–45 min). Baseline spontaneous glutamate release events (glutamate

transients) were measured for 2 min prior to infusion of vehicle. Spontaneous transients were then monitored for 15 min after infusion. Following this, glutamate release was optically evoked by delivery of blue light pulses (473 nm, 5–20 mW, 20 Hz, 5 s or 3 s) to stimulate IOFC or mOFC terminals in the BLA. Each stimulation parameter was repeated three times, with at least 60 s in between stimulations. Rats then received an infusion of CNO (1 mM in 0.5 μ l) into the extracellular space surrounding the MEA. Spontaneous glutamate transients were monitored 2 min before (baseline) and 15 min after CNO infusion. The light delivery protocol was then repeated to assess the effect of CNO:hM4D(Gi) or CNO:mCherry on optically evoked glutamate release from OFC terminals in the BLA. As an iterative control, in a subset of subjects, the applied potential was lowered to 0.2 V, below the H₂O₂ oxidizing potential, and recordings of spontaneous and optically evoked glutamate release were made following CNO infusion.

Optical stimulation. Light was delivered to the BLA via a laser (Dragon Lasers, ChangChun) connected through a ceramic mating sleeve (Thorlabs) to the ferrule implanted on the rat. We used a 473-nm laser to activate OFC terminals expressing ChR2 or a 589-nm laser (largely outside the ChR2 sensitivity range⁵²) as a control for the effects of construct expression and light delivery. For optical stimulation, 25-ms light pulses were delivered at 20 Hz. This frequency was chosen on the basis of previous studies showing reward-induced firing rates for OFC neurons ranging from 6–40 spikes/s^{53,54}. We also found this stimulation frequency to effectively stimulate glutamate release from OFC terminals in the BLA in vivo (Supplementary Fig. 10). Light effects were estimated to be restricted to the BLA on the basis of predicted irradiance values (<https://web.stanford.edu/group/dlab/cgi-bin/graph/chart.php>).

Drug administration. Ifenprodil (Tocris Bioscience) and NBQX (2,3-dioxo-6-nitro-1,2,3,4-tetrahydrobenzo[*f*]quinoxaline-7-sulfonamide disodium salt; Tocris Bioscience) were dissolved in sterile saline vehicle. CNO (Tocris Bioscience) was dissolved in artificial cerebrospinal fluid (aCSF) to a concentration of 1 mM. Drugs were infused bilaterally into the BLA in a volume of 0.5 μ l over 1 min via injectors inserted into the guide cannulae fabricated to protrude 1 mm ventral to the cannula tip by using a microinfusion pump. Injectors were left in place for at least one additional minute to ensure full infusion. This infusion volume was selected to avoid spread to the adjacent central nucleus of the amygdala⁵. Rats were placed in a conditioning chamber 5 min after infusion to allow sufficient time for the drug to become effective. The dose for ifenprodil (1.67 μ g/side), an NMDA receptor antagonist with selective targeting of receptors containing the NR2B subunit¹¹, was selected because it has been shown to impair value-based decision-making⁴. The AMPA receptor antagonist NBQX, at a dose of 1.0 μ g/side, was selected on the basis of our previous evidence of its effectiveness in reward-related tasks^{9,55}. CNO dose was selected on the basis of our previous demonstration of the efficacy and duration of action of this dose and our evidence showing effective inhibition of glutamate release from OFC terminals in the BLA with this dose (Supplementary Fig. 10)¹⁹. We have also demonstrated that this dose of CNO when infused into the BLA has no effect on reward-related behavior in the absence of the hM4D(Gi) transgene¹⁹.

Behavioral procedures. *Apparatus.* Training took place in Med Associates conditioning chambers housed within sound- and light-attenuating boxes, as described previously⁹. For in vivo glutamate measurements, all testing was conducted in a single Med Associates conditioning chamber housed within a continuously connected, copper-mesh-lined sound-attenuating chamber and outfitted with an electrical swivel (Crist Instrument Co.) connecting a headstage tether that extended within the conditioning chamber to the potentiostat recording unit (Fast-16 mkIII, Quanteon) positioned outside the conditioning chamber. For optogenetic experiments, testing was conducted in Med Associates conditioning chambers outfitted with an Intensity Division Fiberoptic Rotary Joint (Doric Lenses) connecting the output fiberoptic patchcords to a laser (Dragon Lasers, ChangChun) positioned outside the conditioning chamber.

All chambers contained two retractable levers that could be inserted into the left and right of a recessed food-delivery port in the front wall. A photobeam entry detector was positioned at the entry to the food port to provide a goal approach measure. The chambers were equipped with a syringe pump to deliver 20% sucrose solution in 0.1-ml increments through a stainless steel tube or a pellet dispenser that delivered a single 45-mg pellet (Bio-Serv) into a custom-designed electrically isolated Acetal plastic well in the food port. A lickometer circuit (Med Associates), connecting the grid floor of the boxes and the stainless steel sucrose-delivery tubes, with the circuit closed by the rat's tongue, allowed recording of lick frequency (licks/s) when rats consumed each sucrose delivery. A 3-W, 24-V house light mounted on top of the back wall opposite the food-delivery port provided illumination.

Training. Each experiment followed the same general structure. Rats were trained on a self-paced two-lever action sequence to earn a delivery of 0.1 ml of 20% sucrose. Training procedures were similar to those we have described previously^{3,56,57}. Except where noted, rats were deprived of food for 4 h prior to each training session. Each session began with illumination of the house light and

insertion of the lever, where appropriate, and ended with retraction of the lever and turning off the house light. Rats were given only one training session per day. Rats received 3 d of magazine training in which they were exposed to noncontingent sucrose deliveries (30 outcomes over 35 min) in the conditioning chamber with the levers retracted, to learn where to receive sucrose. This was followed by daily instrumental training sessions in which sucrose could be earned by lever pressing. Rats were first given 3 d of single-action instrumental training on the lever to the right (the taking lever) of the food-delivery port with the sucrose delivered on a continuous reinforcement schedule. Each session lasted until 20 outcomes had been earned or 30 min had elapsed. Following single-action instrumental training, the seeking lever (the lever to the left of the food-delivery port) was introduced into the chamber. Rats were allowed to press on the seeking lever to gain access to the taking lever, a single press on which delivered the sucrose solution and retracted this lever. The seeking lever remained present during the entire session. Rats were trained on this self-paced two-lever action sequence for a total of 12–18 d: 3 d in which a press on the seeking lever was continuously reinforced with the taking lever, 2–4 d in which the seeking lever was reinforced on a random ratio 2 (RR-2) schedule, 3–5 d in which the seeking lever was reinforced on an RR-5 schedule, and 4–6 d in which the seeking lever was reinforced on the final RR-10 schedule until stable responding was established. The taking lever was always continuously reinforced. Each session lasted until 20 outcomes had been earned or 40 min had elapsed.

Incentive learning opportunity and test. Following training to stable response rates, rats received noncontingent reexposure to the sucrose outcome (30 exposures/35 min) in the conditioning chamber with the levers retracted. Unless otherwise noted, food-port entries and lickometer palatability measures^{58,59} were collected during this phase of the experiment. These noncontingent sucrose deliveries provided an incentive learning opportunity wherein the value of the sucrose could be updated (see specific experimental procedures). Sucrose reexposure was noncontingent to avoid any caching of value to the seeking or taking action. The next day, lever-press behavior was measured during a brief (5-min) nonreinforced probe test to assess the effects of the previous day's incentive learning opportunity on reward-seeking actions. Because no sucrose was delivered during this test, there was no opportunity for online incentive learning or new reinforcement learning. Thus, this task allowed us to experimentally isolate reward value encoding from reward value retrieval.

Online, nearly real-time glutamate detection during sucrose exposure or seeking. Following training on the self-paced action sequence in the sated state (4-h food deprivation) and surgery (Fig. 1a), testing commenced. Prior to each test, rats were placed in the recording conditioning chamber and the biosensor was tethered to the potentiostat via the electrical swivel for application of the 0.7-V potential. The recorded amperometric signal was allowed to stabilize prior to session onset (~30–45 min). First, rats received a single day of instrumental retraining, similar to the training described above but with the ratio requirement progressively increasing from a fixed-ratio-1 to RR-10 after each fifth outcome earned to reestablish lever pressing after surgery. The next day, rats were noncontingently exposed to the sucrose in the familiar sated state (4-h food deprivation) or in a hungry state (20-h food deprivation). For group assignment, subjects were counterbalanced on the basis of average lever-press rate during the last two instrumental training sessions. The next day, all rats were tested hungry. A separate group of rats was maintained hungry throughout training and testing (Supplementary Fig. 5). To prevent electrical interference with the amperometric recordings, lickometers were not connected during recording sessions.

BLA AMPA and NMDA glutamate receptor inactivation during sucrose reexposure or after a reexposure lever-pressing test. Following training in the sated state as described above, drug groups were counterbalanced on the basis of lever-press rate during the two final instrumental training sessions. On two of the instrumental training days immediately prior to the first incentive learning opportunity, rats were given mock infusions to habituate them to the infusion procedures; injectors were inserted into the cannulae but no fluid was infused. All rats then received noncontingent reexposure to sucrose in the hungry state (20-h food deprivation). Prior to this incentive learning opportunity, rats received intra-BLA infusions of vehicle, ifenprodil, or NBQX. The next day, all rats received a drug-free, nonreinforced lever-pressing probe test in the hungry state (Fig. 2a). Following 2 d to reestablish satiety, rats received two sessions of retraining (one session per day) on the action sequence in the 4-h food deprivation state. They were then given another round of reexposure and a lever-pressing test. In this case, noncontingent exposure to the sucrose in the hungry state was conducted without drug. To ensure value encoding and to equate the number of incentive learning opportunities with intact glutamate receptor activity, rats previously assigned to the vehicle group received two drug-free reexposure sessions while rats previously assigned to the ifenprodil or NBQX group received three drug-free reexposure sessions. The day following the last day of reexposure, all rats received a nonreinforced lever-pressing probe test in the hungry state. Prior to this test, rats received an infusion of vehicle, ifenprodil, or NBQX (Fig. 2f). Rats received the same drug on both tests.

Chemogenetic inactivation of IOFC→BLA or mOFC→BLA projections during sucrose reexposure or after a reexposure lever-pressing test. Training and testing were identical to the procedures for the BLA glutamate receptor inactivation experiments except that rats expressing hM4D(Gi) in the IOFC or mOFC received infusion of either vehicle or CNO. All rats received mock infusions to habituate them to the infusion procedures. Following training, rats received noncontingent reexposure to the sucrose in the hungry state (20-h food deprivation). Prior to this incentive learning opportunity, rats received intra-BLA infusions of either vehicle or CNO. The next day, all rats received a drug-free, nonreinforced lever-pressing probe test in the hungry state (Fig. 3a). Following 2 d to reestablish satiety, rats received two sessions of retraining (one session per day) on the action sequence in the 4-h food deprivation state. They were then given another round of reexposure. In this case, noncontingent exposure to the sucrose in the hungry state was conducted without drug. Rats previously assigned to the vehicle group received two drug-free reexposure sessions, while rats previously assigned to the CNO groups received three drug-free reexposure sessions. The day following the last day of reexposure, all rats received a nonreinforced lever-pressing probe test in the hungry state immediately following infusion of either vehicle or CNO into the BLA (Fig. 2g). Drug group assignment for this test was counterbalanced with respect to previous drug treatment. There was no effect of previous drug group ($F_{1,24} = 1.51, P = 0.23$) or interaction between this variable and experimental group ($F_{2,24} = 0.93, P = 0.41$) on reward seeking during the test, indicating that the results of the test were not influenced by drug history. There were no significant differences in reward-seeking lever presses between vehicle-treated subjects expressing hM4D(Gi) in the IOFC as compared to the mOFC during either the first ($t_{11} = 2.00, P = 0.07$) or second ($t_9 = 0.20, P = 0.85$) test, and these groups were therefore collapsed to serve as a single control group.

To evaluate the effect of mOFC→BLA projection inactivation on reward seeking in the absence of reward value retrieval, a separate group of rats expressing hM4D(Gi) in the mOFC was trained while sated and received intra-BLA infusions of vehicle or CNO prior to a nonreinforced lever-pressing probe test in the hungry state as above, but without prior noncontingent reexposure to the sucrose in the hungry state (i.e., without a reward value encoding opportunity; Supplementary Fig. 13). Each rat was given two nonreinforced probe tests, one each following vehicle and CNO infusion for a within-subject drug comparison (test order was counterbalanced). Two days after the last nonreinforced probe test, rats were retrained while sated for 2 d, given a drug-free incentive learning opportunity in the hungry state, and then received intra-BLA infusions of vehicle or CNO prior to a reinforced lever-pressing test (Supplementary Fig. 13). In this test, presence of the sucrose made retrieval of its value from memory unnecessary. Each rat was given two reinforced tests, one each following vehicle and CNO infusion, to allow a within-subject drug comparison (test order was counterbalanced).

Optogenetic activation of OFC→BLA projections during sucrose reexposure. Rats expressing ChR2 or the eYFP control in the IOFC or mOFC with optical fibers above the BLA were trained while sated as described above (Fig. 4a). On the last 2 d of instrumental training, rats were tethered to the patchcord but no light was delivered, to allow habituation to the optical tether. At testing, rats were maintained in the familiar sated state (4-h food deprivation) and received noncontingent reexposure to the sucrose or to a task-irrelevant food pellet. During this noncontingent exposure, blue light (473 nm, 20 Hz, 10 mW, 5 s) was delivered for optical activation of IOFC terminals within the BLA in ChR2-expressing subjects. The laser was triggered by the first lick following sucrose delivery or the first food-port entry following pellet delivery. Optical stimulation timing was based on evidence that BLA glutamate release occurred in response to sucrose consumption during incentive learning and peaked on average 2.79 s (s.e.m. = 0.67 s; range = 0.63–6.1 s) after sucrose collection (Fig. 1d) and evidence that rats finished sucrose consumption and exited the food-delivery port ~5–10 s after reward collection. A subset of rats expressing ChR2 received delivery of 589-nm light (outside the range of ChR2 sensitivity²³) in the BLA. The next day, all rats received a nonreinforced probe test in the familiar sated state while tethered, but without light delivery. This sequence of reexposure and testing was repeated twice, first in a novel moderate-hunger state (8-h food deprivation) and then in a novel hungry state (20-h food deprivation) (Supplementary Fig. 15). Rats were given 2 d off and retrained in the 4-h food deprivation state for 2 d in between each test set. In no case did reward-seeking lever-press activity significantly differ between ChR2-expressing rats that received 589-nm optical activation and eYFP-expressing controls receiving 473-nm optical activation ($t_6 = 0.10–0.95, P = 0.38–0.93$), and these control groups were therefore collapsed to serve as a single control group for each test.

Optogenetic activation of OFC→BLA projections during the lever-pressing test. Rats expressing ChR2 or eYFP in the IOFC or mOFC with optical fibers above the BLA received training, noncontingent sucrose exposure, and testing as described above, except that light (473 nm, 20 Hz, 10 mW, 3 s) was delivered during each of the nonreinforced lever-pressing tests to activate IOFC or mOFC terminals in the BLA in ChR2-expressing subjects. Light was delivered once per minute, for a total of ten light deliveries throughout the 10-min test. The first light delivery occurred 30 s after test onset. The duration of optical stimulation was based on the finding that glutamate release preceded the initiation of reward seeking, and

the rise time to peak glutamate release prior to reward-seeking bouts was on average 1.95 s (s.e.m. = 0.43 s; range = 0.40–3.0 s; Fig. 1f). As above, a subset of ChR2-expressing subjects received delivery of 589-nm light. Tests were conducted with 4, 8, and 20 h of food deprivation, as above, with each lever-pressing test preceded by noncontingent sucrose reexposure in the absence of light delivery. The moderate-hunger state (8-h food deprivation) provided a subthreshold incentive learning opportunity that was, on its own, not sufficiently discriminable to induce an upshift in reward seeking. Reward-seeking presses did not significantly differ between ChR2-expressing rats that received 589-nm light and eYFP-expressing controls receiving 473-nm light ($t_6 = 0.30–2.44, P = 0.051–0.77$), and these groups were therefore collapsed to serve as a single control group for each test.

To examine the effect of mOFC→BLA projection activation on reward seeking in the moderate-hunger state, but in the absence of incentive learning, a separate group of rats expressing ChR2 in the mOFC was trained while sated and received light delivery during a nonreinforced probe test in the moderate-hunger state (8-h food deprivation) as above, but without prior reexposure to sucrose in the 8-h food deprivation state (without the subthreshold incentive learning opportunity). Each rat was given two nonreinforced probe tests, one each with 473-nm light (for ChR2 activation) and 589-nm light (control wavelength), to allow within-subject comparison. Test order was counterbalanced across subjects.

Histology. Rats were transcardially perfused at the conclusion of behavioral testing with PBS followed by 10% formalin. Brains were removed, postfixed in formalin, and then cryoprotected, cut with a cryostat at a thickness of 30 μ m, and collected in PBS. eYFP fluorescence without amplification was used to verify ChR2 expression. To verify hM4D(Gi) expression, immunohistochemical analysis was performed as described previously^{60–62}. Briefly, floating coronal sections were blocked for 1 h at room temperature in 8% normal goat serum (NGS; Jackson ImmunoResearch Laboratories) with 0.3% Triton X-100 in PBS and then incubated overnight at 4°C in 2% NGS, 0.3% Triton X-100 in PBS with primary antibody (anti-HA; 1:500 dilution; BioLegend, cat. no. 901501). Sections were then incubated for 2 h at room temperature with goat anti-mouse IgG, Alexa Fluor 594 conjugate (1:1,000 dilution; Invitrogen, cat. no. A11005). All sections were washed three times for 5 min each in PBS before and after each incubation step and mounted on slides with ProLong Gold antifade reagent with DAPI (Invitrogen). All images were acquired with a Keyence (BZ-X710) microscope with a 4 \times or 20 \times objective (CFI Plan Apo), CCD camera, and BZ-X Analyze software. Biosensor and cannula placements in non-AAV subjects were verified by standard histological procedures.

Data analysis. Behavioral analysis. Seeking and taking lever presses and/or food-port entries were collected continuously for each training and test session. Seeking lever presses were normalized to the baseline response rate averaged across the last two training sessions prior to testing to control for pretest response variability and allow comparison across tests conducted in different deprivation states (see refs. ^{3,56,57,63}). Raw press rate data are presented in the supplemental materials. Lickometer measurements were made during sucrose consumption in the noncontingent reexposure sessions.

Chemogenetic and optogenetic manipulation of glutamate release. Analysis details and characterization of glutamate release events have been described previously^{8,9}. Electrochemical data were baseline subtracted. Detected current was averaged across the first 10 s of the 2-min preinfusion baseline period, and this baseline was subtracted from the current output at each time point. Current changes from baseline on the PPY (or PPD)/Nafion-coated sentinel electrode were then subtracted from current changes on the PPY (or PPD)/Nafion/GluOx-coated glutamate biosensor electrode to remove correlated noise. This signal was then converted to glutamate concentration with an electrode-specific calibration factor obtained *in vitro*. Mini Analysis (Synaptosoft) was used to determine the frequency and amplitude of spontaneous glutamate transient release events. A fluctuation in the glutamate trace was deemed a glutamate transient if it was greater than 2.5 times the root-mean-square noise sampled from the pretest baseline period. To determine transient amplitude, a baseline was taken by averaging three sample bins around the first minima located 0.5–5 s before the peak, and this baseline was subtracted from the peak amplitude. If one peak followed another within 5 s, the baseline was taken after the first peak to distinguish these events. Peaks with a total duration of less than 0.5 s or with an immediately preceding or following negative deflection of amplitude greater than half the peak amplitude were considered noise spikes and were omitted from the analysis. To evaluate optically evoked glutamate release, we isolated the 5-s or 3-s period prior to, during, and following light delivery. The average change in glutamate concentration in the 5-s or 3-s optical stimulation period was subtracted from that during an equivalent period immediately prior to optical stimulation. This was averaged across each of the three replicates for each parameter. There were no statistically significant main effects of OFC subregion (mOFC versus IOFC: $F_{1,4} = 2.09, P = 0.22$; treatment: $F_{1,4} = 8.78, P = 0.04$; brain region \times treatment: $F_{1,4} = 0.01, P = 0.91$), and these data were thus collapsed.

Temporal relationship between glutamate release and behavior. As above, electrochemical data were baseline subtracted. Detected current was averaged

across the 10-s baseline period 2 min prior to testing, and this baseline was subtracted from the current output at each time point. We evaluated the temporal relationship between glutamate release and behavioral events as described previously³⁹. For sucrose reexposure, we isolated changes in glutamate concentration in the 5 s prior to and 10 s following the first food-port entry after each sucrose delivery (reward collection). This period was chosen to give an adequate pre-sucrose baseline and was based on evidence that rats disengaged from the food port ~5–10 s following sucrose collection. The average glutamate concentration in the 1–5 s period 5 s prior to sucrose collection served as the baseline, and this was subtracted from each data point in the peri-sucrose glutamate concentration versus time trace. To quantify the sucrose-evoked change in glutamate concentration, for each trial, the average change in glutamate concentration in the 10-s post-sucrose period was averaged across trials and this was compared to the average change in glutamate concentration in the 5 s prior to sucrose collection and to equivalent analysis of glutamate concentration changes in 5-s periods in the absence of sucrose or checking behavior.

During the nonreinforced lever-pressing probe test, because rats tended to organize their reward-seeking lever presses into bouts, we focused on presses that initiated bouts of reward-seeking activity (initiating presses), excluding presses that occurred within a pressing bout, as we have described previously⁹. An 'initiating seeking press' was defined as the first press after completion of an action sequence or, because rats often disengaged from the lever and then reinitiated reward seeking, the first press after a >6-s pause in pressing. Similar definitions of initiation of reward seeking and instrumental bouts defined by pauses in activity have been described previously^{36,64}. See Supplementary Table 2 for seeking bout information. We evaluated changes in glutamate concentration in the 5 s prior to and following each initiating reward-seeking press. The average glutamate concentration in the 1-s period 5 s prior to each initiating press served as the baseline. This analysis window was selected to avoid contaminating events (for example, termination of a previous bout, food-port entries, etc.). The average change in glutamate concentration for each initiating press was quantified in the 3-s periods immediately prior to and after each initiating press, and this was compared to equivalent analysis of changes in glutamate concentration in the absence of lever pressing. Data were averaged across trials. We quantified glutamate concentration around all intra-bout seeking presses similarly (Supplementary Fig. 6). Pearson correlations were used to assess the relationship between glutamate fluctuations around bout initiation and the number of presses and duration of subsequent bouts.

Palatability analysis. A lickometer circuit (Med Associates), connecting the grid floor of the box and the stainless steel sucrose-delivery tubes, with the circuit closed by the rat's tongue, allowed recording of individual lick events. Lickometer measures were amplified and fed through an interface to a PC programmed to record the time of each lick to the nearest millisecond. On the basis of previous reports^{3,63,65}, we used licking frequency (licks/s) as a measure of sucrose palatability. This measure of licking microstructure during consumption provides a similar analysis of palatability changes as assessing taste reactivity following oral infusions³⁸. These data were analyzed with custom-written Python-based code.

Statistical analysis. Datasets were analyzed by two-tailed Student's *t* test or by one- or two-way repeated-measures ANOVA, as appropriate. Bonferroni-corrected post hoc tests were performed to clarify all main effects and interactions. Two-tailed paired *t* tests were used for a priori planned comparisons, as advised by ref. ⁶⁶, on the basis of a logical extension of Fisher's protected least significant difference (PLSD) procedure for controlling familywise type I error rates. No statistical methods were used to predetermine sample sizes, but our sample sizes are similar to those reported in previous publications^{3,56,57,63}. Investigators were not blinded in glutamate receptor antagonist or chemogenetic experiments because they were required to administer drug. The behavioral experimenter was blinded to viral conditions in optogenetic experiments. All data were tested for normality and all datasets met assumptions of equal covariance, justifying ANOVA interpretation⁶⁷. Alpha levels were set at $P < 0.05$.

Reporting Summary. Further information on research design is available in the Nature Research Reporting Summary linked to this article.

Data availability

All data that support the findings of this study are available from the corresponding author upon reasonable request.

Code availability

Custom-written Python-based code is available from the corresponding author upon request.

References

- Wassum, K. M. et al. Silicon wafer-based platinum microelectrode array biosensor for near real-time measurement of glutamate in vivo. *Sensors* **8**, 5023–5036 (2008).
- Zhang, F. et al. Multimodal fast optical interrogation of neural circuitry. *Nature* **446**, 633–639 (2007).
- Schoenbaum, G., Chiba, A. A. & Gallagher, M. Neural encoding in orbitofrontal cortex and basolateral amygdala during olfactory discrimination learning. *J. Neurosci.* **19**, 1876–1884 (1999).
- van Duuren, E. et al. Neural coding of reward magnitude in the orbitofrontal cortex of the rat during a five-odor olfactory discrimination task. *Learn. Mem.* **14**, 446–456 (2007).
- Feltenstein, M. W. & See, R. E. NMDA receptor blockade in the basolateral amygdala disrupts consolidation of stimulus-reward memory and extinction learning during reinstatement of cocaine-seeking in an animal model of relapse. *Neurobiol. Learn. Mem.* **88**, 435–444 (2007).
- Wassum, K. M., Cely, I. C., Balleine, B. W. & Maidment, N. T. Micro-opioid receptor activation in the basolateral amygdala mediates the learning of increases but not decreases in the incentive value of a food reward. *J. Neurosci.* **31**, 1591–1599 (2011).
- Wassum, K. M., Greenfield, V. Y., Linker, K. E., Maidment, N. T. & Ostlund, S. B. Inflated reward value in early opiate withdrawal. *Addict. Biol.* **21**, 221–233 (2016).
- Davis, J. D. & Perez, M. C. Food deprivation- and palatability-induced microstructural changes in ingestive behavior. *Am. J. Physiol.* **264**, R97–R103 (1993).
- Berridge, K. C. Modulation of taste affect by hunger, caloric satiety, and sensory-specific satiety in the rat. *Appetite* **16**, 103–120 (1991).
- Malvaez, M. et al. HDAC3-selective inhibitor enhances extinction of cocaine-seeking behavior in a persistent manner. *Proc. Natl Acad. Sci. USA* **110**, 2647–2652 (2013).
- Malvaez, M., Mhillaj, E., Matheos, D. P., Palmery, M. & Wood, M. A. CBP in the nucleus accumbens regulates cocaine-induced histone acetylation and is critical for cocaine-associated behaviors. *J. Neurosci.* **31**, 16941–16948 (2011).
- Malvaez, M., Sanchis-Segura, C., Vo, D., Lattal, K. M. & Wood, M. A. Modulation of chromatin modification facilitates extinction of cocaine-induced conditioned place preference. *Biol. Psychiatry* **67**, 36–43 (2010).
- Wassum, K. M., Ostlund, S. B., Balleine, B. W. & Maidment, N. T. Differential dependence of Pavlovian incentive motivation and instrumental incentive learning processes on dopamine signaling. *Learn. Mem.* **18**, 475–483 (2011).
- Wassum, K. M., Ostlund, S. B., Loewinger, G. C. & Maidment, N. T. Phasic mesolimbic dopamine release tracks reward seeking during expression of Pavlovian-to-instrumental transfer. *Biol. Psychiatry* **73**, 747–755 (2013).
- Kaplan, J. M., Roitman, M. F. & Grill, H. J. Ingestive taste reactivity as licking behavior. *Neurosci. Biobehav. Rev.* **19**, 89–98 (1995).
- Levin, J. R., Serlin, R. C. & Seaman, M. A. A controlled powerful multiple-comparison strategy for several situations. *Psychol. Bull.* **115**, 153–159 (1994).
- Tabachnick, B. G., Fidell, L. S. & Osterlind, S. J. *Using Multivariate Statistics* 4th edn (Allyn and Bacon, 2001).

Reporting Summary

Nature Research wishes to improve the reproducibility of the work that we publish. This form provides structure for consistency and transparency in reporting. For further information on Nature Research policies, see [Authors & Referees](#) and the [Editorial Policy Checklist](#).

Statistics

For all statistical analyses, confirm that the following items are present in the figure legend, table legend, main text, or Methods section.

- | n/a | Confirmed |
|-------------------------------------|--|
| <input type="checkbox"/> | <input checked="" type="checkbox"/> The exact sample size (n) for each experimental group/condition, given as a discrete number and unit of measurement |
| <input type="checkbox"/> | <input checked="" type="checkbox"/> A statement on whether measurements were taken from distinct samples or whether the same sample was measured repeatedly |
| <input type="checkbox"/> | <input checked="" type="checkbox"/> The statistical test(s) used AND whether they are one- or two-sided
<i>Only common tests should be described solely by name; describe more complex techniques in the Methods section.</i> |
| <input checked="" type="checkbox"/> | <input type="checkbox"/> A description of all covariates tested |
| <input type="checkbox"/> | <input checked="" type="checkbox"/> A description of any assumptions or corrections, such as tests of normality and adjustment for multiple comparisons |
| <input type="checkbox"/> | <input checked="" type="checkbox"/> A full description of the statistical parameters including central tendency (e.g. means) or other basic estimates (e.g. regression coefficient) AND variation (e.g. standard deviation) or associated estimates of uncertainty (e.g. confidence intervals) |
| <input type="checkbox"/> | <input checked="" type="checkbox"/> For null hypothesis testing, the test statistic (e.g. F , t , r) with confidence intervals, effect sizes, degrees of freedom and P value noted
<i>Give P values as exact values whenever suitable.</i> |
| <input checked="" type="checkbox"/> | <input type="checkbox"/> For Bayesian analysis, information on the choice of priors and Markov chain Monte Carlo settings |
| <input checked="" type="checkbox"/> | <input type="checkbox"/> For hierarchical and complex designs, identification of the appropriate level for tests and full reporting of outcomes |
| <input type="checkbox"/> | <input checked="" type="checkbox"/> Estimates of effect sizes (e.g. Cohen's d , Pearson's r), indicating how they were calculated |

Our web collection on [statistics for biologists](#) contains articles on many of the points above.

Software and code

Policy information about [availability of computer code](#)

Data collection

Med-Associates Med-PC custom code was used to collect behavioral data, Quanteon 1.0 FAST software was used for amperometry data collection

Data analysis

All data were processed using Microsoft Excel 2013 (Redmond, WA), then compiled and statistically analyzed with GraphPad Prism v6.07 (La Jolla, CA) and SPSS v24 (IBM Corp, Chicago, IL). A custom-written python script was used for lickometer data analysis, synaptosoft mini analysis v6.0.7 was used for glutamate transient analysis.

For manuscripts utilizing custom algorithms or software that are central to the research but not yet described in published literature, software must be made available to editors/reviewers. We strongly encourage code deposition in a community repository (e.g. GitHub). See the Nature Research [guidelines for submitting code & software](#) for further information.

Data

Policy information about [availability of data](#)

All manuscripts must include a [data availability statement](#). This statement should provide the following information, where applicable:

- Accession codes, unique identifiers, or web links for publicly available datasets
- A list of figures that have associated raw data
- A description of any restrictions on data availability

All data that support the findings of this study are available from the corresponding author.

Field-specific reporting

Please select the one below that is the best fit for your research. If you are not sure, read the appropriate sections before making your selection.

Life sciences Behavioural & social sciences Ecological, evolutionary & environmental sciences

For a reference copy of the document with all sections, see [nature.com/documents/nr-reporting-summary-flat.pdf](https://www.nature.com/documents/nr-reporting-summary-flat.pdf)

Life sciences study design

All studies must disclose on these points even when the disclosure is negative.

Sample size	The number of animals proposed per group was informed by power analyses performed on previously-collected data to generate group sizes that will ensure minimally sufficient statistical power (0.9) to detect statistically significant differences between groups (0.05), using mixed ANOVA and appropriate post-hoc tests adjusted for multiple comparisons. Sample size also included expected attrition due to misplaced fibers/cannula and virus.
Data exclusions	Data was excluded if biosensor, cannula, viral expression, or optic fiber placement was off-target. The criteria were established prior to data collection and reported in the Methods section.
Replication	All experiments were run in at least 2 cohorts of subjects for internal replication. All attempts at replication were successful.
Randomization	For deprivation state and drug group assignments, subjects were counterbalanced based on the average lever-press rate during the last two instrumental training session. For viral vector infusions, two weeks prior to behavioral procedures, rats were randomly assigned to viral group
Blinding	Investigators were not blinded in glutamate receptor antagonist or chemogenetic experiments because they were required to administer drug. Behavioral experimenter was blinded to viral conditions in optogenetic experiments.

Reporting for specific materials, systems and methods

We require information from authors about some types of materials, experimental systems and methods used in many studies. Here, indicate whether each material, system or method listed is relevant to your study. If you are not sure if a list item applies to your research, read the appropriate section before selecting a response.

Materials & experimental systems

n/a	Involvement in the study
<input type="checkbox"/>	<input checked="" type="checkbox"/> Antibodies
<input checked="" type="checkbox"/>	<input type="checkbox"/> Eukaryotic cell lines
<input checked="" type="checkbox"/>	<input type="checkbox"/> Palaeontology
<input type="checkbox"/>	<input checked="" type="checkbox"/> Animals and other organisms
<input checked="" type="checkbox"/>	<input type="checkbox"/> Human research participants
<input checked="" type="checkbox"/>	<input type="checkbox"/> Clinical data

Methods

n/a	Involvement in the study
<input checked="" type="checkbox"/>	<input type="checkbox"/> ChIP-seq
<input checked="" type="checkbox"/>	<input type="checkbox"/> Flow cytometry
<input checked="" type="checkbox"/>	<input type="checkbox"/> MRI-based neuroimaging

Antibodies

Antibodies used	anti-HA, 1:500, Biolegend, San Diego, CA, cat. no. 901501, lot:B220768 goat anti-mouse IgG, Alexa 594 conjugate, 1:1000, Invitrogen, cat. no. A11005, Lot: GR303504-1
Validation	anti-HA has been validated by manufacturer using immunofluorescence and immunoprecipitation. Relevant citations can be found on manufacturer's website: https://www.biolegend.com/en-us/products/purified-anti-ha-11-epitope-tag-antibody-11374 goat anti-mouse IgG, Alexa 594 conjugate relevant citations can be found on manufacturer's website: https://www.thermofisher.com/antibody/product/Goat-anti-Mouse-IgG-H-L-Cross-Adsorbed-Secondary-Antibody-Polyclonal/A-11005

Animals and other organisms

Policy information about [studies involving animals](#); [ARRIVE guidelines](#) recommended for reporting animal research

Laboratory animals	Male, Long Evans rats (aged 8-10 weeks at the start of the experiment; Charles River Laboratories, Wilmington, MA) were used.
Wild animals	This study did not involve wild animals.

Field-collected samples

This study did not involve samples collected from the field.

Ethics oversight

All procedures were conducted in accordance with the NIH Guide for the Care and Use of Laboratory Animals and were approved by the UCLA Institutional Animal Care and Use Committee.

Note that full information on the approval of the study protocol must also be provided in the manuscript.